CROWN BIOSCIENCE

Tumor Homograft Models

Combine the predictive power of GEMM with consistent, robust allograft models for pharmacological research

A JSR Life Sciences Company

FACTSHEET

V1.0

While GEMM are highly useful for mechanism of action studies, the spontaneous nature of their tumors makes them less suitable for studying the efficacy of oncology and immunooncology agents.

To combine the rich, diverse genotypes and phenotypes of available GEMM with an improved operational simplicity, Crown Bioscience has developed the tumor homograft platform:

- Mouse allograft models derived from GEMM or carcinogen-induced model tumors
- Engrafted in immunocompetent mice
- For efficient efficacy testing of novel agents and combination treatments including immunotherapies
- Featuring tumors which are primary in nature, and mirror original tumor histopathology and genetic profiles, maintained permanently *in vivo*
- Models feature reduced variability compared with traditional syngeneic models
- Wide range of cancer types available, many featuring highly relevant mutations for targeted immunotherapy development.

Crown Bioscience provides a range of mouse allograft models for preclinical efficacy testing:

- Mouse allograft models derived from GEMM or carcinogen-induced tumors, engrafted in mice with complete immunocompetency to assess novel oncology or immuno-oncology agents, including targeted therapies
- These models recapitulate their original tumor for a range of features including genotypes and phenotypes, microenvironments, and cancer stem cell driven disease
- Combine the diverse selection of GEMM models (including tumors with a clear molecular pathogenesis of disease) with the operational simplicity needed for pharmacological assessment
- Wide range of cancer types available, including bladder, brain, breast, head and neck, lung, lymphoma, pancreatic, prostate, sarcoma, and skin cancer
- Includes models with oncogenic mutations e.g. KRAS G12D

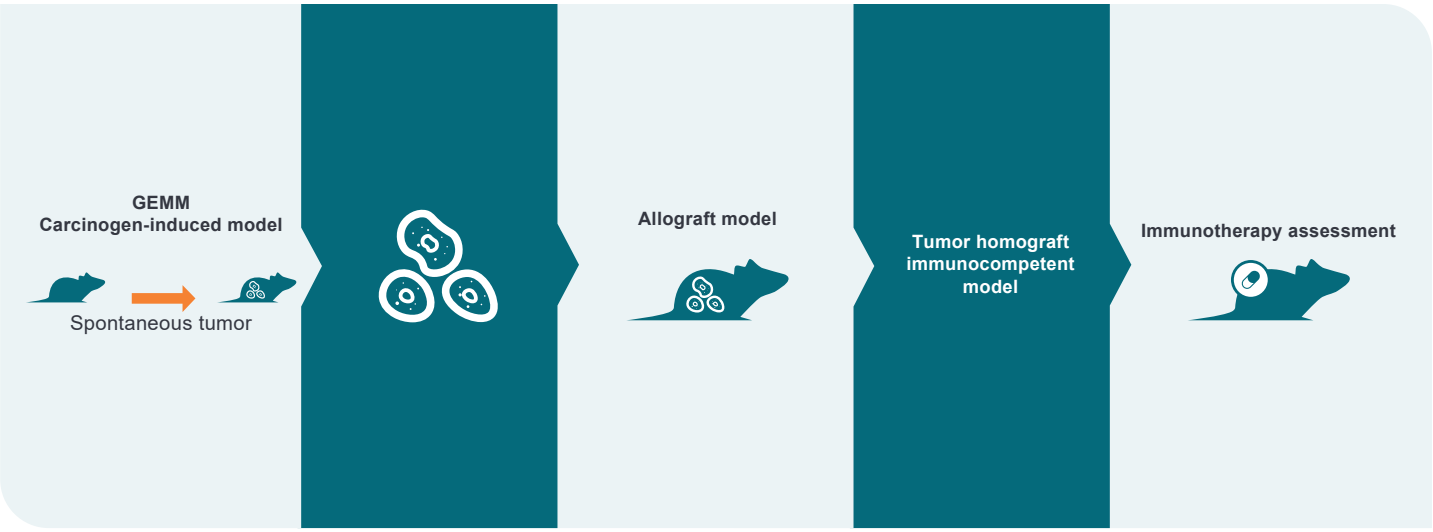

Mouse Allograft Models – A GEMM-Derived Efficacy Testing Platform

As immunotherapies continue to bring treatment breakthroughs across a range of cancer types, improved preclinical models are required for novel agent assessment, including models with fully functional immunity.

Immunocompetent, genetically engineered mouse models (GEMM) have been a long used research tool. While they are highly useful for monitoring cancer progression and mechanism of action studies, the spontaneous nature of GEMM tumors makes them complex and costly models for efficacy studies.

With the wide variety of well-characterized GEMM available (featuring tumors with a clear molecular pathogenesis of disease) generating libraries of mouse allograft models using GEMM tumors has become highly useful to researchers. Similar to patient-derived xenograft (PDX) models, murine libraries are primary in nature, mirror the original tumor histopathology and genetic profile, but also provide an improved operational simplicity needed for efficacy studies[1].

MuPrime Background and Concept

Tumor homografts are the murine version of PDX. These models are comprised of allografts of spontaneous murine tumors derived from GEMM or carcinogen-induced models, studied in mice with complete immunocompetency (Figure 1).

Similar to to the parental models, the tumor lines have never been manipulated or adapted to grow in vitro, replicating original mouse tumor genotypes and phenotypes, with different differentiation phenotypes, rich microenvironments, and cancer stem cell driven disease[1].

The collection covers a wide diversity of cancer types, and enables preclinical research into, and discovery of, specific pathways and predictive biomarkers for targeted immunotherapy agents. It combines the improved predictive power of GEMM with an operational consistency and ease of use, as well as robust growth for pharmacology research.

The data from our models are all stored within our easy to use, free to access, proprietary database IO Murine Models. A wide variety of data including model background, mouse strain, histopathology, genomic profiling (RNAseq), standard of care (SoC), and immunoprofiling (infiltrating immune cells, cytokine profile, response to checkpoint inhibitors, etc.) data are also captured in the database. This allows researchers to quickly and easily search for models of interest to meet their research needs.

The collection contains a range of highly characterized models across a variety of cancer types. One of our most highly characterized and SoC validated models, mBR6004(2) with MMTV-PyVT TG mutation, is fully detailed within our standalone mBR6004 Factsheet.

This includes full model background, histopathology QC of the parental GEMM vs tumor homograft model, mutation status via RNAseq (mutations found in EGFR, HER2, and MET), IHC (confirming ER- and HER2 3+), gene expression via RNAseq, growth rates, SoC treatment data, and lung metastasis data. Immuno-oncology profiling is also included within the Factsheet to confirm levels of TILs following treatment with anti-PD-1 and anti-CTLA-4 therapies, together with treatment data for these antibodies.

Figure 1: Concept and Building the Library

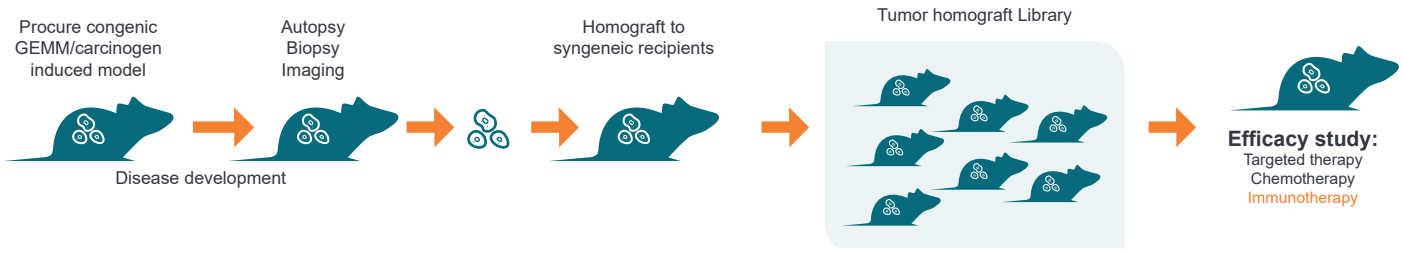

Tumor homograft Immunotherapy Model Collection

Our pipeline is shown in Table 1.

Table 1: Model Collection

Model	Cancer Type; Biopsy Site	Mutations/Carcinogen	Strain Background	Pathology QC
mBL6078	Bladder; bladder (near the suture)	KRAS (G12D); $PTEN^{Flox/Flox}$	C57BL/6	Synovial sarcoma (Pa)
mBN6091	Brain; brain	KRAS LSL(G12D)/WT; $PTEN^{CKO/CKO}$	C57BL/6	Glioblastoma (P1)
mBR6004	Breast; breast	MMTV-PyVT TG	FVB/N	Papillary adenocarcinoma (Pa)
mHN6032	Head and neck; ventral neck region	NA	BALB/c	Neuroendocrine carcinoma (P2)
mLU6044	Lung; lung	KRAS (G12D); $P53^{-/-}$	C57BL/6	Moderately differentiated adenocarcinoma (P0, P4)
mLU6045	Lung; lung	KRAS (G12D); $P53^{-/-}$	C57BL/6	Poorly to moderately differentiated adenocarcinoma (Pa, P5)
mLU6050	Lung; lung	Urethane	BALB/c	Moderately differentiated adenocarcinoma (P1, P2)
mLU6051	Lung; lung	Urethane	BALB/c	Papillary adenocarcinoma (P0), poorly differentiated adenocarcinoma (Pa)
mLU6054	Lung; lung	KRAS (G12D); $PTEN^{Flox/Flox}$	C57BL/6	Moderately differentiated adenocarcinoma (P0)
mLU6073	Lung; lung	$PTEN^{Flox/Flox}$; $P53^{-/-}$	C57BL/6	Osteosarcoma (Pa, P1)
mLU6075	Lung; lung	$P53^{-/-}$	C57BL/6	Osteosarcoma (Pa), undifferentiated sarcoma (P2), synovial sarcoma (P2)
mLU6081	Lung; lung	Urethane	A/J	Papillary adenocarcinoma (P1), moderately to poorly differentiated adenocarcinoma (Pa)
mLU6131	Lung; lung	Urethane	A/J	Moderately differentiated adenocarcinoma (P1), neuroendocrine carcinoma (Pa)
mLU6132	Lung; lung	Urethane	A/J	Moderately to poorly differentiated adenocarcinoma (P0, Pa)
mLU6133	Lung; lung	Urethane	A/J	Papillary adenocarcinoma (Pa)
mLU6134	Lung; lung	Urethane	A/J	Moderately to poorly differentiated adenocarcinoma (Pa), papillary adenocarcinoma (P1
mLY6014	Lymphoma; ventral neck region	NA	NOD/ShiLt	Diffuse large B cell lymphoma (DLBCL) (P5)
mLY6041	Lymphoma; right side of neck	KRAS (G12D); $P53^{-/-}$	C57BL/6	DLBCL (Pa, P5)
mLY6043	Lymphoma; thymus	IgH-Myc TG (Eμ Myc)	C57BL/6	DLBCL (Pa, P4)
mLY6061	Lymphoma; NA	KRAS LSL(G12D)WT;$P53^{-/-}$	C57BL/6	DLBCL (P1, P3)
mLY6062	Lymphoma; thymus	KRAS LSL(G12D)WT;$P53^{-/-}$	C57BL/6	DLBCL (P1, P3)
mLY6068	Lymphoma; thymus, thyroid, and axillary lymph nodes	IgH-Myc TG (Eμ Myc)	C57BL/6	Undifferentiated sarcoma (Pa), DLBCL with hemorrhagic necrosis (P4)
mLY6096	Lymphoma; mesentery	IgH-Myc TG (Eμ Myc)	C57BL/6	Burkitt's lymphoma (P4, Pa)
mLY6097	Lymphoma; dorsal side of foreleg	IgH-Myc TG (Eμ Myc)	C57BL/6	Burkitt's lymphoma (Pa), DLBCL (P5)

Model	Cancer Type; Biopsy Site	Mutations/Carcinogen	Strain Background	Pathology QC
mLY6098	Lymphoma; thyroid	IgH-Myc TG (Eμ Myc)	C57BL/6	DLBCL (Pa, P3)
mLY6101	Lymphoma; thymus	IgH-Myc TG (Eμ Myc)	C57BL/6	Burkitt's lymphoma (P4, Pa)
mLY6102	Lymphoma; axillary lymph nodes of foreleg	IgH-Myc TG (Eμ Myc)	C57BL/6	Burkitt's lymphoma (Pa), DLBCL (P5)
mLY6149	Lymphoma; right side of scapula	IgH-Myc TG (Eμ Myc)	C57BL/6	DLBCL with massive necrosis (P3, Pa)
mLY6150	Lymphoma; thyroid	IgH-Myc TG (Eμ Myc)	C57BL/6	DLBCL with massive necrosis (P0, P5)
mLY6166	Lymphoma; right side of scapula	IgH-Myc TG (Eμ Myc)	C57BL/6	DLBCL with massive necrosis (Pa)
mLY6167	Lymphoma; mesentery	IgH-Myc TG (Eμ Myc)	C57BL/6	DLBCL with massive necrosis (P3, Pa)
mLY6168	Lymphoma; thymus	IgH-Myc TG (Eμ Myc)	C57BL/6	DLBCL (Pa), mantle cell lymphoma (P2)
mLY6169	Lymphoma; thyroid	IgH-Myc TG (Eμ Myc)	C57BL/6	Mantle cell lymphoma (P3, Pa)
mPA6059	Pancreatic; pancrea	KRAS (G12D); $P53^{-/-}$	C57BL/6	High grade spindle cell sarcoma (P0), poorly differentiated squamous cell carcinoma (P3)
mPA6063	Pancreatic; pancrea	KRAS (G12D); $P53^{-/-}$	C57BL/6	High grade undifferentiated sarcoma (Pa, P2)
mPA6114	Pancreatic; pancrea	KRAS (G12D); $P53^{-/-}$	C57BL/6	Moderately differentiated adenocarcinoma (P5, Pa)
mPA6115	Pancreatic; pancrea	KRAS (G12D); $P53^{-/-}$	C57BL/6	Moderately differentiated adenocarcinoma (P6, Pa)
mPR6003	Prostate; prostate	TRAMP (Pbsn-SV40T) TG	C57BL/6	Moderately differentiated adenocarcinoma (Pa), prostate cancer (P0)
mPR6065	Prostate; prostate	PTENFlox/Flox; $P53^{-/-}$	C57BL/6	LipoSA-Sarcoma (P2)
mPR6066	Prostate; prostate	PTENFlox/Flox; $P53^{-/-}$	C57BL/6	LipoSA-Sarcoma (P1)
mPR6135	Prostate; prostate	KRAS (G12D); $PTEN^{Flox/Flox}$; Probasin-cre	C57BL/6	Sarcoma
mSA6046	Sarcoma; duodenum	KRAS (G12D); $P53^{-/-}$	C57BL/6	Undifferentiated sarcoma (Pa, P5)
mSA6048	Sarcoma; enterocoelia (near the suture)	KRAS (G12D); P53-/-	C57BL/6	Undifferentiated sarcoma (Pa, P5)
mSA6055	Lung; lung	KRAS (G12D); $PTEN^{Flox/Flox}$	C57BL/6	Osteosarcoma (P1, P6, Pa)
mSA6084	Sarcoma; enterocoelia (near the suture)	KRAS (G12D); $PTEN^{Flox/Flox}$	C57BL/6	Osteosarcoma (P1, Pa)
mSA6105	Sarcoma; dorsal side of foreleg	$PTEN^{Flox/Flox}$; $P53^{-/-}$	C57BL/6	Undifferentiated sarcoma (Pa, P1)
mSA9003	Sarcoma; dorsal side of foreleg	$P53^{-/-}$	C57BL/6	Malignant peripheral nerve sheath tumor (P1)
mSK6005	Skin; dorsal side of foreleg	$Apc^{Min/+}$	C57BL/6	Well differentiated squamous cell carcinoma (P0)
mXX6127	Unclear	Urethane	C3H/He	Papillary adenocarcinoma (P6, Pa)
mXX6129	Unclear	Urethane	C3H/He	Papillary adenocarcinoma (Pa), neuroendocrine carcinoma (P2)

mSK6005 Skin Cancer Model

A further highly characterized model is the mSK6005 skin cancer model, developed from $APC^{Min/+}$ mice. Heterozygous $APC^{Min/+}$ mice are highly susceptible to intestinal adenoma[3,4]; however, female $APC^{Min/+}$ mice also occasionally develop mammary squamous cell carcinomas[5].

We observed a spontaneous cutaneous tumor on the neck of the C57BL/6J $APC^{Min/+}$ mouse, which histopathology suggests to be a welldifferentiated skin squamous cell carcinoma, and from which we have developed the mSK6005 skin cancer model (Table 1)[6]. The mSK6005 model grows robustly, with serial transplants of the model maintaining the histopathology of the primary tumor (Table 2).

Immunoprofiling, RNA sequencing, and treatment with standard of care agents and immunotherapies have also been completed for this model.

Transcriptome sequencing shows that the mSK6005 model maintains the original APC^{Min} mutation (nonsense mutation L850*), and has frameshift mutations present in: c-Met (frameshift insertion 901G>GA) and EGFR (frameshift insertion 1431G>GA) [6]. The model also expresses high levels of HER2 (Table 3).

In vivo pharmacological assessment shows that the mSK6005 model responds to SoC chemotherapies (Figure 2):

- 5-FU
- paclitaxel
- gemcitabine
- gemcitabine
- cisplatin[6].

The model is also sensitive to an anti-mouse CTLA-4 antibody (Figure 3).

Table 2: mSK6005 Model Histopathology

MuPrime ID	Pathology	Histopathology	
		Pa	P0
mSK6005	Skin cancer, squamous cell carcinoma	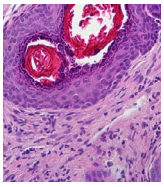	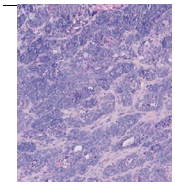

H&E stained pathology images from the original GEMM primary tumor (Pa) and from an early passage of the model (P0).

Table 3: mSK6005 Model Immunohistochemistry: HER2

IHC Target	HER2
mSK6005	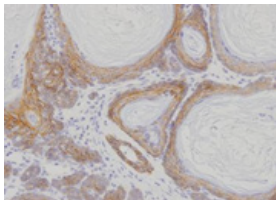

Expression of HER2 was confirmed using a polyclonal antibody against an intracellular domain of HER2 (Dako).

Figure 2: mSK6005 Model Responds to SoC

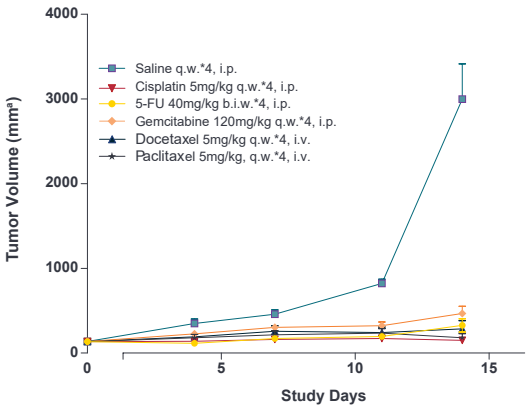

Figure 3: mSK6005 Model Responds to Anti-CTLA-4 Treatment

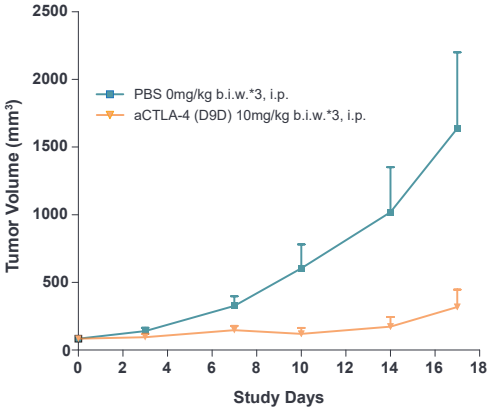

KRAS G12D GEMM-Derived Models

Crown Bioscience has derived tumor homograft models from tumors which feature the KRAS G12D mutation, across a range of cancer types including bladder, lung, pancreas, and lymphoma (as detailed in Table 1). These models include mPA6115, a KPC mouse homograft model of pancreatic ductal adenocarcinoma (PDAC)[7,8], which retains morphological similarity to human PDAC (Figure 4), and which is a highly useful tool for immunotherapy and targeted agent evaluation. The mPA6115 model can be both subcutaneously and orthotopically engrafted as required.

Baseline immunoprofiling identified tumor-infiltrating immune cells of different subsets in both orthotopic and subcutaneously implanted tumors, with profiles differing for the two engraftment types (Figure 5). Highly enriched CD45+ lymphocytes, particularly B cells and macrophages, were observed in the tumor

The orthotopic and subcutaneous models demonstrate similar growth rates and a lack of response to standard of care gemcitabine treatment (Figure 6).

Figure 4: mPA6115 Model Histopathology

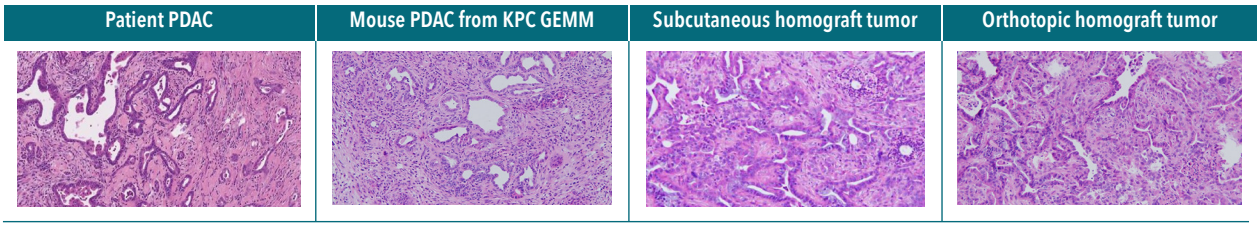

Figure 5: mPA6115 Model Baseline Immunoprofiling

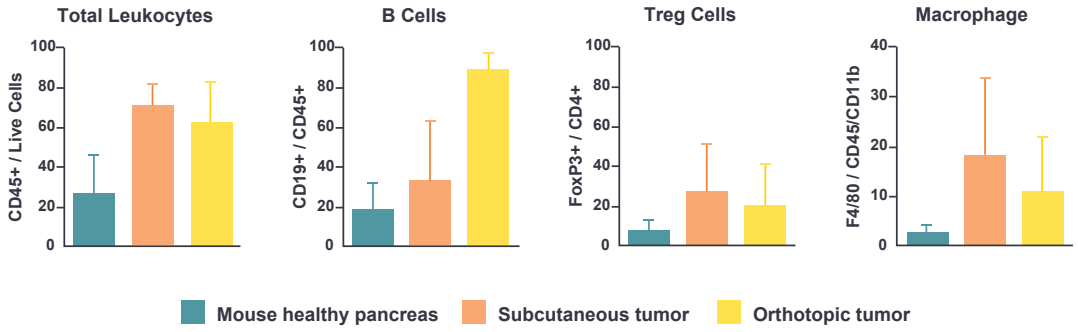

Figure 6: mPA6115 Model Does Not Responds to Gemcitabine Treatment

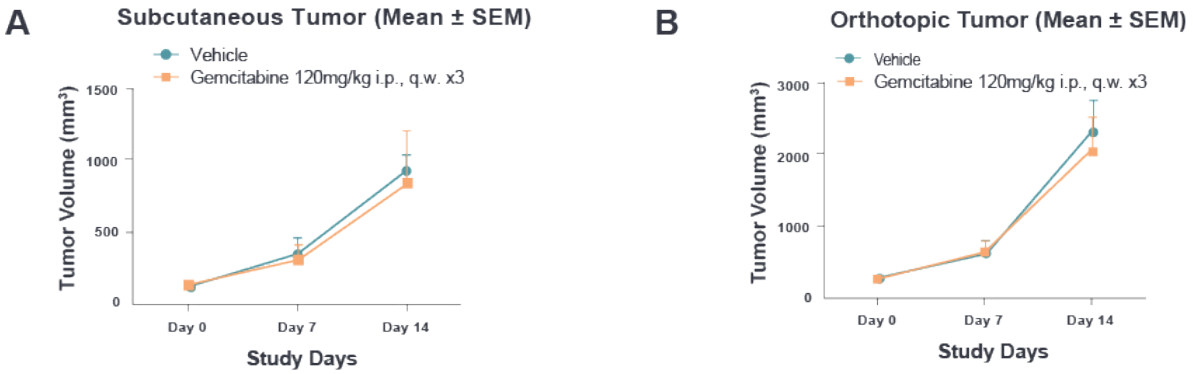

A: subcutaneous tumor; B: orthotopic tumor.

Summary

Immunotherapy agents are showing considerable success in oncology; providing both patient benefits and commercial success for the pharmaceutical industry. However, progress in the field is hindered through a lack of experimental immunotherapy models featuring a fully competent immune system.

Crown Bioscience provides a range of immuno-oncology platforms for preclinical drug development, including tumor homograft models. This platform comprises of allografts of spontaneous murine tumors derived from GEMM or carcinogen-induced models, engrafted in immunocompetent mice, which have never been manipulated or adapted to grow *in vitro*.

The tumor homograft platform enables preclinical research into specific pathways and predictive biomarkers for targeted immunotherapy agents, with a greater operational simplicity than GEMM/carcinogen-induced models.

Tumor homograft models are available for use across a variety of cancer types with an extensive pipeline in development. Available models have been validated through a range of genomic profiling, pathology, IHC, and FACS analyses, and we have a range of SoC and immunotherapy data available, providing models to suit all research needs.

References

[1] Li QX, Feuer G, Ouyang X *et al*. Experimental animal modeling for immuno-oncology. *Pharmacology & Therapeutics* 2017;173:34-46.

[2] Wang Z, An X, Liu J *et al*. Response to Checkpoint Inhibition by GEMM Breast Cancer Allograft. [abstract]. In: Proceedings of the AACR-NCI-EORTC International Conference: Molecular Targets and Cancer Therapeutics; 2015 Nov 5-9; Boston, MA. Philadelphia (PA): AACR; *Molecular Cancer Therapeutics* 2015;14(12 Suppl 2):Abstract nr B97.

[3] Moser AR, Pitot HC, Dove WF. A dominant mutation that predisposes to multiple intestinal neoplasia in the mouse. *Science* 1990;247(4940): 322-324.

[4] Su LK, Kinzler KW, Vogelstein B *et al*. Multiple intestinal neoplasia caused by a mutation in the murine homolog of the APC gene. *Science* 1992;256(5057): 668-670.

[5] Moser AR, Hegge LF, Cardlff RD. Genetic background affects susceptibility to mammary hyperplasias and carcinomas in Apc(min)/+ mice. *Cancer Research* 2001;61(8): 3480-3485.

[6] Qu GJ, An AX, Liu J *et al*. Establishment of a mouse skin squamous cell carcinoma allograft model for *in vivo* pharmacological analysis of immunotherapy [abstract]. In: Proceedings of the 107th Annual Meeting of the American Association for Cancer Research; 2016 Apr 16-20; New Orleans, LA. Philadelphia (PA): AACR; *Cancer Research* 2016;76(14 Suppl):.Abstract nr 4043.

[7] Tong L, Song Y, Liu B *et al*. Establishment of Kras (G12D)/ Trp53 null/Pdx1-cre (KPC) mouse homograft tumor models to facilitate preclinical efficacy evaluation of combinatory immunotherapies [abstract]. In: Proceedings of the 4th AACR New Horizons in Cancer Research Conference: Research Propelling Cancer Prevention and Cures; 2017 Nov 6-9; Shanghai, China. Abstract nr A63.

[8] An X, Ouyang X, Zhang H *et al*. Immunophenotyping of orthotopic homograft (syngeneic) of murine primary KPC pancreatic ductal adenocarcinoma by flow cytometry. *Journal of Visualized Experiments*; 2018:in press.

Get in touch

Sales
US: +1 858 622 2900
UK: +44 (0)1530 234871
busdev@crownbio.com
www.crownbio.com